

Non-adiabatic polaron hopping conduction in semiconducting V_2O_5 – Bi_2O_3 oxide glasses doped with $BaTiO_3$

S. CHAKRABORTY, M. SADHUKHAN, D. K. MODAK, B. K. CHAUDHURI
Solid State Physics Department, Glass and Ceramic Section, Indian Association for the Cultivation of Science, Calcutta 700 032, India

$BaTiO_3$ -doped (5–40 wt %) $90V_2O_5$ – $10Bi_2O_3$ (VB) glasses have been prepared by a quick quenching technique. The d.c. electrical conductivities, $\sigma_{d.c.}$, of these glasses have been reported in the temperature range 80–450 K. The electrical conductivity of these glasses, which arises due to the presence of V^{4+} and V^{5+} ions, has been analysed in the light of the small-polaron hopping conduction mechanism. The adiabatic hopping conduction valid for the undoped VB glasses (with 80–95 mol % V_2O_5), in the high-temperature region, is changed to a non-adiabatic hopping mechanism in the $BaTiO_3$ -doped VB glasses. At lower temperatures, however, a variable range hopping (VRH) mechanism dominates the conduction mechanism in both the glass systems. Such a change-over from adiabatic to non-adiabatic conduction mechanism is a new feature in transition metal oxide glasses. Various parameters, such as density of states at the Fermi level $N(E_F)$, electron wave-function decay constant, α , polaron radius, r_p , and its effective mass, m_p^* , etc., have been obtained for all the glass samples from a critical analysis of the electrical conductivity data satisfying the theory of polaron hopping conduction.

1. Introduction

Recently, many transition metal oxide semiconducting (TMOS) glasses with V_2O_5 , Cu_2O , Fe_2O_3 , etc., have been studied [1–4] because of their possible applications as optical switching and memory devices [5–9], cathode materials in battery applications [10], and ferrites [11], etc. Among these, vanadate glasses with glass-former oxides such as P_2O_5 , TeO_2 and SiO_2 , etc., have been widely studied. The pure vanadate glasses are found to absorb moisture from the atmosphere and hence are unstable. However, the vanadate glasses formed with Bi_2O_3 , Sb_2O_3 , GeO_2 , etc., are found to be quite stable [4, 12] and they are suitable for technological applications as threshold and memory-switching devices [7–9]. The semiconducting behaviour of these TMO glasses arises due to two different valence states (e.g. V^{4+} and V^{5+} in vanadate glasses). The electrical conduction is due to the hopping of electrons (or polarons) from lower to higher valence state [13]. The effect of doping ferroelectric ($BaTiO_3$) or piezoelectric (ZnO) substances in TMO glasses, such as V_2O_5 – Bi_2O_3 has not been well studied. However, semiconducting $BaTiO_3$ grains, separated from each other by insulating layers, have been used to develop barrier layer capacitors [14]. A remarkable feature of the $BaTiO_3$ -doped V_2O_5 – Bi_2O_3 glasses is that their permittivity [15] is of the order of 10^4 (or more depending on the $BaTiO_3$ concentrations) which is possible when fine par-

ticles/clusters of $BaTiO_3$ are present in the glass network [16]. This behaviour of the $BaTiO_3$ -doped glasses is quite different from that of the pure V_2O_5 – Bi_2O_3 glasses or other TMOS glasses studied earlier, where dielectric permittivity is comparatively small and is not suitable for use as capacitor materials. Therefore, it is interesting to study the electrical properties of the $BaTiO_3$ -doped glasses and to compare them with those of the pure V_2O_5 – Bi_2O_3 glass system.

The main objective of the present work was to investigate the electrical properties (d.c. conductivity denoted by $\sigma_{d.c.}$) of the $BaTiO_3$ -doped $90V_2O_5$ – $10Bi_2O_3$ glasses for a wide range of $BaTiO_3$ concentrations. It was observed that the electrical conductivities of these glasses are much smaller than those of the undoped V_2O_5 – Bi_2O_3 glasses and can be well explained by the small-polaron theory which shows a change-over from adiabatic (in V_2O_5 – Bi_2O_3 glasses) to non-adiabatic (in $BaTiO_3$ -doped glasses) hopping conduction process.

2. Experimental procedure

The starting base glass, $90V_2O_5$ – $10Bi_2O_3$ (VB), and the $BaTiO_3$ -doped (VB + $xBaTiO_3$) glasses (VBBT) with $x = 5, 10, 15, 20, 30$ and 40 wt % VB were prepared by a quick quenching technique, similar to that in our earlier works [4, 17]. The oxide materials, V_2O_5 , Bi_2O_3 , $BaTiO_3$ (grain size 1.8–2 μm), used in

TABLE I Chemical compositions, density, average site spacing, and phonon frequency of the $90\text{V}_2\text{O}_5-10\text{Bi}_2\text{O}_3-x\text{BaTiO}_3$ glasses^a. The values of ν_{ph} are obtained from the fitting of the $\sigma_{\text{d.c.}}$ data

x (wt %)	Density (g cm^{-3})	T_g ($^{\circ}\text{C}$)	N (10^{21} cm^{-3})	V^{4+} (10^{20} cm^{-3})	$C = V^{4+}/V_t$ ($V_t = V^{4+} + V^{5+}$)	R (nm)	ν_{ph} (10^{13} Hz)
5	4.108	234	5.04	6.15	0.122	0.583	1.15
10	4.195	246	4.92	5.86	0.119	0.588	1.06
15	4.287	250	4.81	5.48	0.114	0.593	0.95
20	4.378	275	4.70	5.12	0.109	0.597	1.04
30	4.560	286	4.52	4.75	0.105	0.605	0.91
40	4.773	312	4.39	3.91	0.089	0.611	0.90

^a Maximum errors in the estimations of T_g , ρ and C are, respectively, $\pm 2^{\circ}\text{C}$, $\pm 0.05 \text{ g cm}^{-3}$ and ± 0.02 .

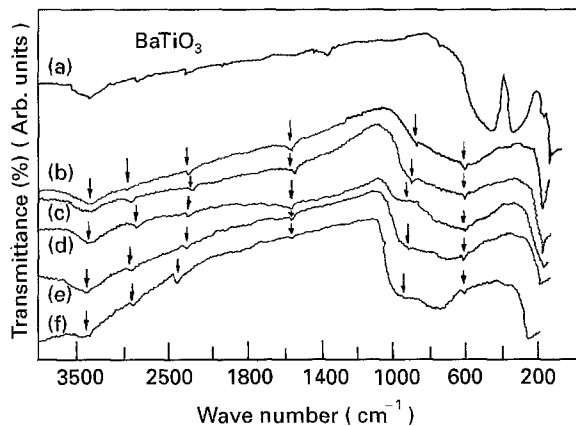


Figure 1 Infrared absorption spectra of crystalline BaTiO_3 powder used for glass making (a) and $90\text{V}_2\text{O}_5-10\text{Bi}_2\text{O}_3-x\text{BaTiO}_3$ glasses at room temperature with $x =$ (b) 5, (c) 10, (d) 20, (e) 30 and (f) 40 wt % BaTiO_3 . The peak around 480 cm^{-1} (a) is a characteristic peak of BaTiO_3 which is absent in the present glasses of our investigation.

the preparation of the glasses were of 99.99% purity. All the glasses were prepared by quenching from their respective melts at $900-1100^{\circ}\text{C}$ (depending upon BaTiO_3 concentrations) between two copper blocks. Each melt was kept at these temperatures for 2 h. The glassy character of all the samples was confirmed [15] by X-ray diffraction (Philips, Model PW1710) and scanning electron microscopy studies (Model 415A, Hitachi, Japan). The density of the glasses (measured using Archimedes' principle), as shown in Table I, was found to increase almost linearly with BaTiO_3 concentration. The differential thermal analysis of the samples was performed (Model Shimadzu DT-30) at a heating rate of $10^{\circ}\text{C min}^{-1}$. The glass transition temperature, T_g , of the samples, given in Table I, was also found to increase with increasing BaTiO_3 content in the glass. The energy dispersive X-ray analysis indicated that the ratio V:Bi:Ba:Ti was in agreement with the mixing compositions. The infrared absorption studies of all these glasses are very similar, as shown in Fig. 1, for some of these glasses. All the glass samples exhibited a water band at $\sim 3400 \text{ cm}^{-1}$. The peak at about 605 cm^{-1} corresponds to the phonon frequency, ν_{ph} , of about $1.8 \times 10^{13} \text{ Hz}$, which agreed with that measured from the electrical conductivity data, as discussed in Section 3.

For electrical measurements, the glass plates were cut, polished and gold plated by a sputtering technique. The method of measuring the d.c. conductivity

(between 80 and 450 K) was as discussed elsewhere [17]. Each datum was taken giving sufficient time (30–40 min) for temperature stability. The concentration of V^{4+} and V^{5+} ions for all the samples was determined by redox titration of the solution of the samples against potassium permanganate solution [18], similar to our earlier works [4, 7–9]. These results have been found to agree, within $\pm 5\%$, with those obtained from the electron paramagnetic resonance (e.p.r.) studies [19] (Model Joel, RE1X, Japan). Detailed results of e.p.r. studies will be published elsewhere. Table I shows the values of V^{4+}/V_{total} ($V_{\text{total}} = V^{4+} + V^{5+}$) ratio obtained from chemical analysis, together with other data.

3. Results and discussion

The d.c. conductivities, $\sigma_{\text{d.c.}}$ of the $\text{VB} + x\text{BaTiO}_3$ (VBBT) glasses as a function of inverse temperature are shown in Fig. 2. It is observed that the d.c. conductivity varies smoothly with $1000/T$, showing a temperature-dependent activation energy, W . Such a behaviour is typical of small polaron hopping conduction in TMO glasses [13, 16, 19, 20]. The inverse temperature dependence of $\sigma_{\text{d.c.}}$ for the $\text{V}_2\text{O}_5-\text{Bi}_2\text{O}_3$ glasses is also shown in Fig. 3 for comparison. The $\sigma_{\text{d.c.}}$ value at any fixed temperature (say 300 K) decreases with increasing BaTiO_3 concentration in the glasses (Fig. 4). Above 250–300 K, depending on the compositions of the glasses, the conductivity is almost linear with inverse temperature. The activation energies of the VBBT glasses, estimated at 330 K and 140 K from Fig. 2, are shown in Table II. It was found that activation energy increases with increase of BaTiO_3 concentration. In the $\text{V}_2\text{O}_5-\text{Bi}_2\text{O}_3$ glasses, the activation energy increases with increase of Bi_2O_3 (cf. [4]). The activation energy obtained for the VB glass is also reported in Table II for comparison.

It is further observed that the current intensity in the VBBT glasses, after the application of a fixed voltage, remains constant with time. This implies that the electrical conduction in these glasses is electronic in nature, which is also confirmed from the measurement of thermoelectric power at ambient temperature.

The well-known [20] expression for small polaron hopping conduction in semiconducting glasses is

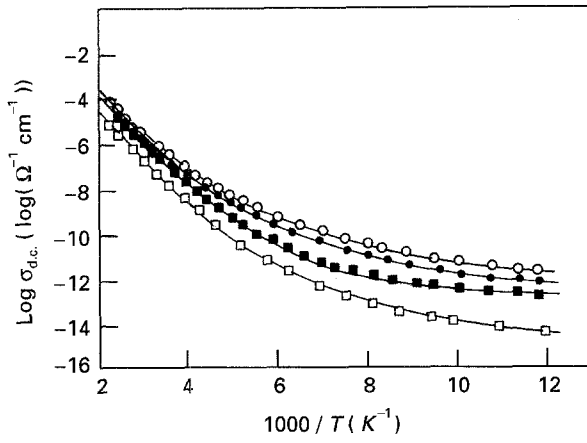


Figure 2 Logarithm of d.c. conductivity versus $1/T$ for different values of x (wt %) of BaTiO_3 the $90\text{V}_2\text{O}_5-10\text{Bi}_2\text{O}_3-x\text{BaTiO}_3$ glasses. x : (○) 10, (●) 20, (■) 30, (□) 40 wt %.

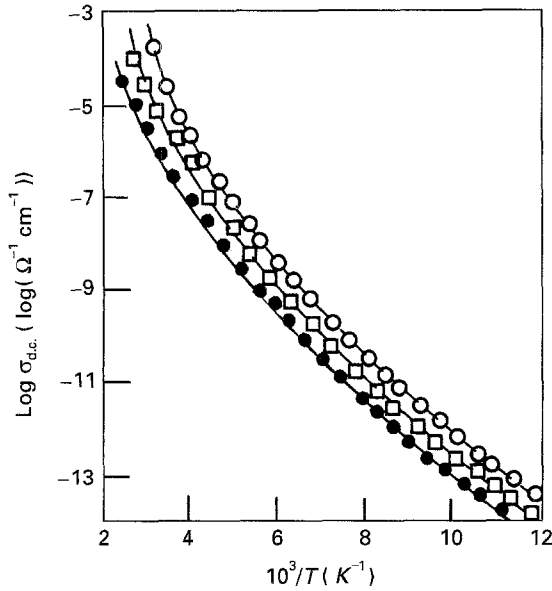


Figure 3 Logarithm of d.c. conductivity versus $1/T$ for (○) $95\text{V}_2\text{O}_5-5\text{Bi}_2\text{O}_3$, (□) $90\text{V}_2\text{O}_5-10\text{Bi}_2\text{O}_3$ and (●) $80\text{V}_2\text{O}_5-20\text{Bi}_2\text{O}_3$ glasses.

given by

$$\sigma_{d.c.} = v_{ph} e^2 R^2 N \beta C (1 - C) \exp(-2\alpha R) \exp(-W/KT) \quad (1)$$

where v_{ph} is the optical phonon frequency, N is the number of transition metal ion sites per unit volume, R is the average site spacing, C is the ratio of the ion

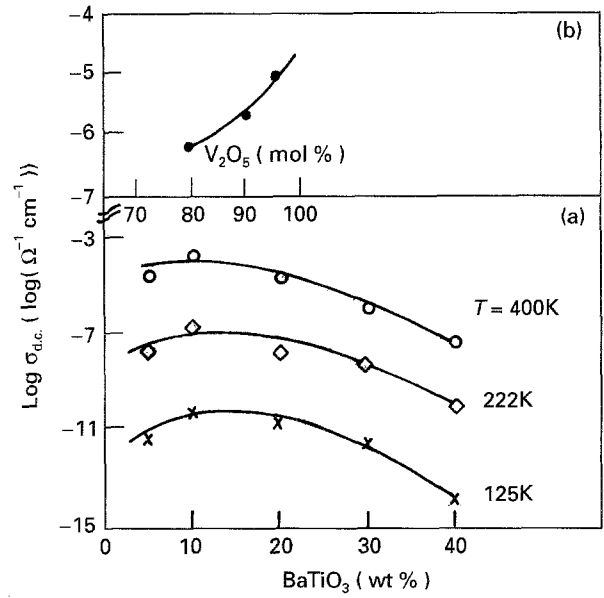


Figure 4 The variation of d.c. conductivity of (a) the $90\text{V}_2\text{O}_5-10\text{Bi}_2\text{O}_3-x\text{BaTiO}_3$ glasses with BaTiO_3 concentration (x) at three fixed temperatures, and (b) $\text{V}_2\text{O}_5-\text{Bi}_2\text{O}_3$ glasses with concentration of V_2O_5 at 300 K.

concentration in the low valency state to the total concentration of transition metal ions (Table I), α is the electron wave function decay constant, so that $\exp(-2\alpha R)$ represents electron overlap between sites, W is the activation for conduction and $\beta = 1/k_B T$ (k_B is the Boltzmann's constant and T is the absolute temperature). Assuming strong electron-phonon interaction. Austin and Mott [13] showed that

$$W = W_H + W_D/2 \quad (\text{for } T > \theta_D/2) \quad (2a)$$

$$W = W_D \quad (\text{for } T < \theta_D/4), \quad (2b)$$

where W_H is the polaron hopping energy and W_D is the disorder energy arising from the energy differences of the neighbouring sites. The Debye temperature, θ_D , is defined by $h\nu_{ph} = K_B \theta_D$ (where k_B is Boltzmann's constant). The importance of the tunnelling term $\exp(-2\alpha R)$ in Equation 1 for the present system of glasses could be understood by plotting $\log \sigma_{d.c.}$ against W at a chosen temperature for all the VBBT glasses (Fig. 5). The temperature T_e (say), estimated from the slope of such a plot, would be close to the experimental temperature when hopping is considered in the adiabatic regime [21]. On the other hand, T_e would be very different from the experimental

TABLE II Some important model parameters for $90\text{V}_2\text{O}_5-10\text{Bi}_2\text{O}_3-x\text{BaTiO}_3$ glasses obtained by best fitting of the conductivity data

BaTiO ₃	ϵ_p	W (eV)		W_H (eV)	$\frac{\Delta W}{W_{300K} - W_H}$	r_p (nm)	
		140 K	330 K			Eq. 4	Eq. 5
0	6.50	0.080	0.301	0.210	0.091	0.141	0.263
5	6.25	0.121	0.286	0.146	0.140	0.235	0.241
10	6.05	0.122	0.296	0.150	0.146	0.237	0.250
15	5.91	0.124	0.300	0.152	0.148	0.239	0.259
20	5.76	0.126	0.350	0.155	0.195	0.241	0.267
30	5.66	0.144	0.356	0.156	0.200	0.244	0.278
40	5.57	0.174	0.421	0.157	0.264	0.246	0.282

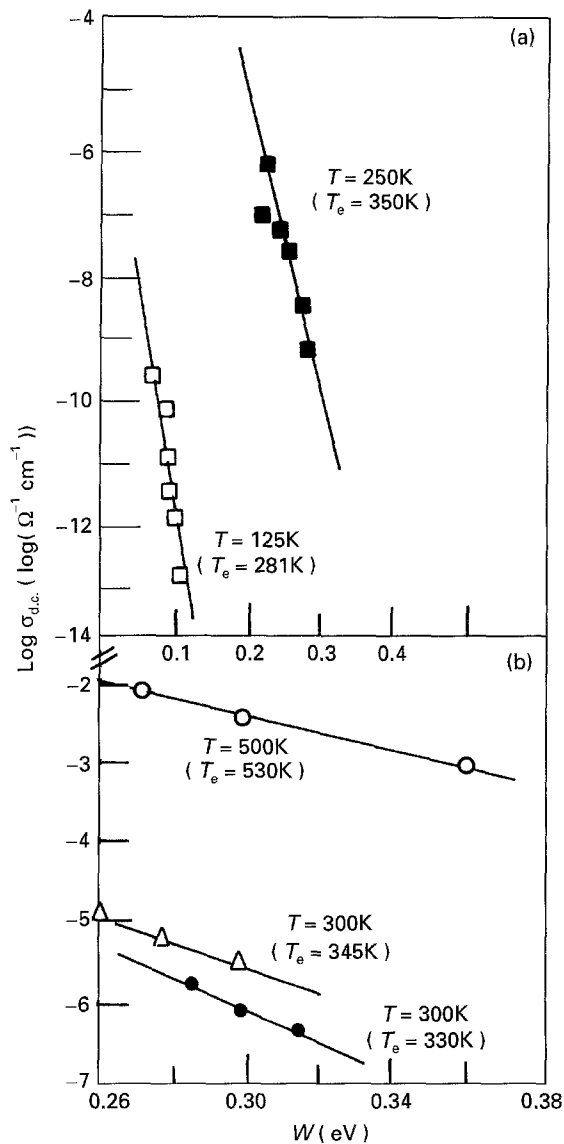


Figure 5 (a) The logarithm of d.c. conductivity versus activation energy, W , for the $90\text{V}_2\text{O}_5-10\text{Bi}_2\text{O}_3-x\text{BaTiO}_3$ glasses. The open values of temperature correspond to the experimental temperatures while the temperatures within the parenthesis correspond to the values estimated from the slopes. Here experimental temperatures and the corresponding temperatures obtained from the slopes, T_e , are quite different. (b) The logarithm of conductivity versus activation energy curves for three vanadate glasses showing the adiabatic hopping conduction mechanism. (○) $\text{V}_2\text{O}_5-\text{P}_2\text{O}_5$, (△) $\text{V}_2\text{O}_5-\text{TeO}_2$, and (●) the present base glass $\text{V}_2\text{O}_5-\text{Bi}_2\text{O}_3$. For all these samples, experimental temperatures, T , and the temperature, T_e , estimated from the corresponding slopes, are almost equal.

temperature if the hopping is considered in the non-adiabatic regime. Such a plot for two chosen temperatures ($T = 125$ and 250 K) is shown in Fig. 5a for VBBT glasses. The temperatures, T_e , estimated from the slopes of the curves of Fig. 5a are 281 and 350 K, respectively, which are somewhat larger than the corresponding chosen temperatures. Similar curves drawn for the $\text{V}_2\text{O}_5-\text{Bi}_2\text{O}_3$, $\text{V}_2\text{O}_5-\text{P}_2\text{O}_5$, and $\text{V}_2\text{O}_5-\text{TeO}_2$ glasses [4] in Fig. 5b indicate that the experimental temperature and the T_e values are quite close to each other for all the glass systems. Thus, the higher values of T_e from the corresponding experimental temperatures for the VBBT glasses suggest non-adiabatic polaron hopping conduction, while for the $\text{V}_2\text{O}_5-\text{Bi}_2\text{O}_3$, $\text{V}_2\text{O}_5-\text{P}_2\text{O}_5$ and $\text{V}_2\text{O}_5-\text{TeO}_2$

glasses, the adiabatic hopping conduction mechanism is valid. The general conclusion that may be drawn from Fig. 5a and b is that the pre-exponential term in Equation 1, inclusive of $\exp(-2\alpha R)$, is virtually constant for all vanadate glasses. The thermal activation energy for conduction, therefore, appears to dominate the factors that determine the conductivity in this glass system. In particular, the tunnelling term $\exp(-2\alpha R)$ need not be assumed to vary rapidly with the site spacing, R , in order to explain the variation in the conductivity for the VB glasses. Many TMOS glasses [21] (except $\text{Bi}_2\text{O}_3-\text{Fe}_2\text{O}_3$ [22, 23], where the conduction mechanism is non-adiabatic) behave in this manner. Here we should mention that for all the multicomponent Bi-Sr-Ca-Cu-O-type glassy precursors for high T_c superconductors, the conduction mechanism is non-adiabatic [24]. For the VBBT-type glasses, where the non-adiabatic hopping mechanism is valid, the tunnelling term is found to be very important. The presence of BaTiO_3 in the VB glasses is responsible for the change-over from the adiabatic to non-adiabatic small polaron hopping regime in the present VBBT glass system.

The small polaron model [13] predicts that an appreciable departure from a linear plot of $\sigma_{d.c.}$ against $1/T$ should occur below a temperature $\theta_D/2$. Figs 2 and 3 also show that a temperature-dependent activation energy is observed only below about 250 K. Thus the small polaron model provides an estimate for $\theta_D/2$ of about 250 K. The estimated phonon frequency for all the glasses in our investigation is of the order of 10^{13} Hz, as shown in Table I. The characteristic phonon frequency estimated from the infrared spectra (Fig. 1) is found to be of the order of 1.8×10^{13} Hz, corresponding to an infrared band around 605 cm^{-1} . Therefore, the values of phonon frequency estimated from the small polaron theory (Table I) are close to the optical phonon frequency estimated from infrared studies. It is worthwhile noting that the infrared spectra of different compositions of the VBBT glasses are very similar (Fig. 1), suggesting that the optical phonon distribution does not differ appreciably between different compositions of the glasses.

It is interesting to estimate the decay constant, α , from the high-temperature electrical conductivity data using Equation 1. For this purpose, $\log(\sigma_{d.c.} T)$ is plotted against $1/T$ in Fig. 6 for different VBBT glasses. The lines in Fig. 6 are obtained by the least squares fitting method. The pre-exponential factor in Equation 1 obtained by this fitting procedure is shown in Table I. The values of α are obtained from $\exp(-2\alpha R)$ using known values of the parameters of Table I. It is observed from Table III that the values of α calculated for various glass compositions, indicate strong localization in these glasses. For the VBBT glasses under study, the values of α lie within the limits suggested by Austin and Garbett [25] for the TMO glasses. For the calculation of polaron binding energy, W_p , Holstein [26, 27] derived the relation

$$W_p = (2N)^{-1} \sum |\gamma_q|^2 \hbar v_q / 2\pi \quad (3)$$

where γ_p is the electron-phonon coupling constant and v_q is the frequency of optical phonons with wave

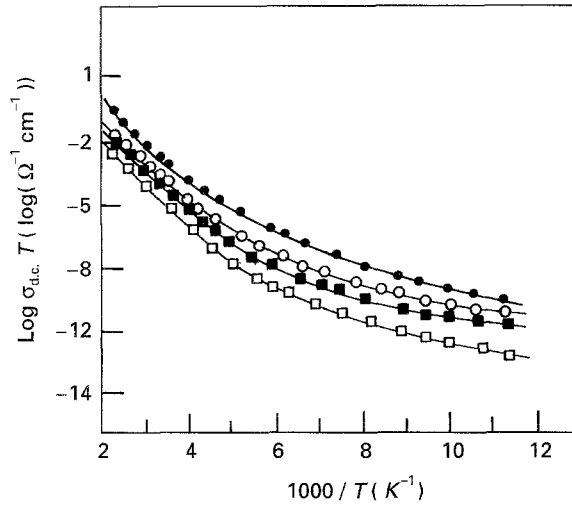


Figure 6 The variation of $\log(\sigma_{d.c.} T)$ with inverse temperature for the $90V_2O_5-10Bi_2O_3-xBaTiO_3$ glasses. x : (●) 10, (○) 20, (■) 30, (□) 40 wt %.

number q , and N is the site concentration. Austin and Mott [13] have also derived a more direct expression, namely

$$W_p = (e^2/\epsilon_p r_p)/2 \quad (4)$$

where r_p is the polaron radius and ϵ_p is an effective dielectric constant given by $1/\epsilon_p = 1/\epsilon_\alpha - 1/\epsilon_s$ (where ϵ_α and ϵ_s are the high-frequency and static dielectric constants, respectively).

Bogomolov *et al.* [28] showed that Equation 4 can also be derived from Equation 3 for a non-dispersive system of frequency ν_{ph} . The polaron radius is given by

$$r_p = 1/2(\pi/6)^{1/3} R \quad (5)$$

The value of r_p calculated from Equation 5 using the average value of site spacing, R (from Table I), are shown in Table II. An experimental estimation [13] of r_p , as obtained from Equation 4 taking

$$W \approx W_H = W_{p/2} = (e^2/4\epsilon_p)(1/r_p - 1/R) \quad (6)$$

is also shown in Table II. The value ϵ_p is found from the refractive indices of the glasses ($\epsilon_p = \epsilon_\alpha = n^2$, where n is the refractive index) and n varies from 2.35–2.55 as determined from the measurement of Brewster's angles. The estimated polaron radius, r_p , is found to be less than the average site spacing, R , suggesting small polaron formation in these glasses.

The disorder energy, W_D , is calculated from Miller and Abraham's theory [29] using the relation $W_D = 0.3\epsilon^2/\epsilon_s R$. The values of static dielectric constants, ϵ_s , are estimated from the dielectric constants measurements [15]. We notice that the values of $\Delta W (= W - W_H)$ at 330 K vary in the range 0.14–0.26 eV (depending upon $BaTiO_3$ concentrations shown in Table II) which is much higher than the theoretically calculated values of $W_D/2$. Similar results have also been observed for $Bi_2O_3-Fe_2O_3$ (cf. [22, 23]) and vanadate glasses [3]. This discrepancy might be due to the differences in the microstructures of the glass network.

At low temperatures, where the polaron binding energy is small and the static disorder energy plays a dominant role in the conduction mechanism, Mott [20] has suggested a variable range hopping process. The conductivity for the variable range hopping is given by

$$\sigma_{d.c.} = A \exp(-B/T^{1/4}) \quad (7)$$

where A and B are constants and B is given by

$$B = 2.1 [\alpha^3/k_B N(E_F)]^{1/4} \quad (8a)$$

$$B = 2.4 [W_D(\alpha R)^3/k_B]^{1/4} \quad (8b)$$

where $N(E_F)$ is the density of states at Fermi level. Fig. 7a shows a plot of $\log \sigma_{d.c.}$ as a function of $T^{-1/4}$ for different VBBT glasses under study. It is interesting to note that there are actually two distinct straight lines with different slopes above and below 102 K. For the VB glass this value is about 100 K (Fig. 7b). From the slopes of the curves, the values of α and W_D have been calculated using Equation 8 taking $N(E_F) = 1 \times 10^{19} \text{ eV}^{-1} \text{ cm}^{-3}$ as obtained from fitting of the a.c. conductivity data with the overlapping large polaron tunnelling model [19]. Here, too, the values of α (Table III) reside within the limit suggested by Austin and Garbett [25], but the calculated values of W_D (using Equation 8b) are unacceptably large. This type of large value has also been reported earlier [3, 22, 23] for many TMOS glasses.

As mentioned above, information about the nature of hopping conduction in the VBBT glasses can also be obtained from Holstein's condition [26, 27, 30]. The polaron band width, ΔE_J , should satisfy the inequality

$$\Delta E_J \geq (2k_B T W_H/\pi)^{1/4} (h\nu_{ph}/\pi)^{1/2} \quad (9)$$

TABLE III Some important model parameters (α , γ_p and ΔE_J) for the $90V_2O_5-10Bi_2O_3-xBaTiO_3$ glasses obtained from fitting of the experimental d.c. conductivity data

x (wt %)	$\alpha(\text{nm}^{-1})^a$	γ_p	ΔE_J (eV)	m_p/m^*
0	12.70 (28.9)	14.0	0.2930	1.20×10^6
5	6.92 (1.3)	7.05	0.0110	0.12×10^4
10	6.87 (3.0)	7.24	0.0116	0.14×10^4
15	6.02 (1.4)	7.39	0.0120	0.16×10^4
20	4.72 (1.8)	7.49	0.0125	0.18×10^4
30	4.40 (2.0)	7.50	0.0128	0.19×10^4
40	2.76 (4.4)	7.60	0.0132	0.20×10^4

^a The values of α are calculated from $\nu_{ph} \exp(-2\alpha R)$ knowing $\nu_{ph} = 10^{13}$ Hz and R (shown in Table I) and the corresponding values of α within the brackets are obtained from Mott's $T^{-1/4}$ analysis (Equation 8)

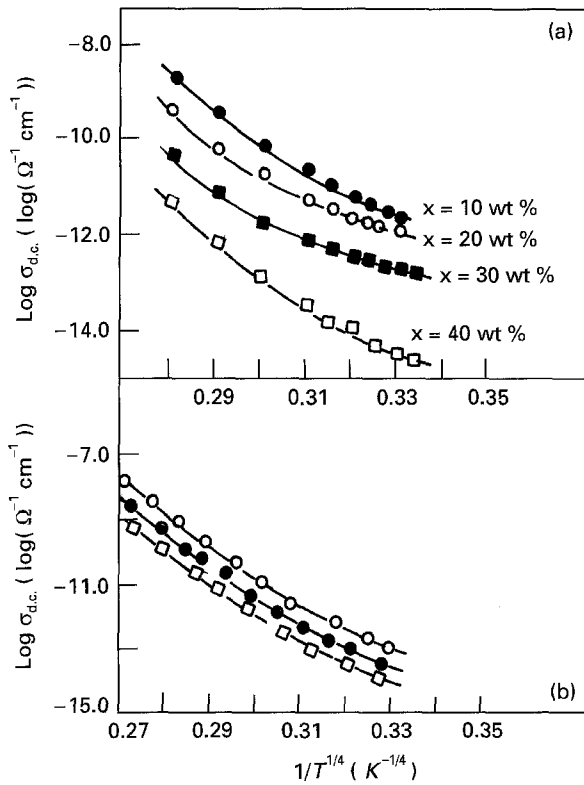


Figure 7 Plot of $\log \sigma_{d.c.}$ as a function of $1/T^{1/4}$ at low temperatures for (a) the $90V_2O_5-10Bi_2O_3-xBaTiO_3$ glasses, and (b) the $V_2O_5-Bi_2O_3$ glasses for different mol % Bi_2O_3 : (○) 4.8, (●) 9.7, (□) 19.5.

where the greater than sign indicates hopping in the adiabatic regime, and the less than sign indicates hopping in the non-adiabatic regime, respectively. Further, the condition for the formation of a small polaron is $\Delta E_j \leq W_H/3$. Now, from the estimated values of W_H and ΔE_j listed in Table II and III, respectively, we find that this condition is satisfied for the VBBT glasses, suggesting the existence of small polarons.

The value of ΔE_j can be estimated from the approximate relation derived by Mott and Davis [31], namely

$$\Delta E_j \approx e^3 [N(E_F)/\epsilon_p^3]^{1/2} \quad (10)$$

Putting the values of ϵ_p from Table II and taking $N(E_F) = 10^{19} \text{ eV}^{-1} \text{ cm}^{-3}$ (as obtained from the a.c. conductivity data for the VBBT glasses [19]), the values of ΔE_j lie in the range 0.011–0.013 eV for the VBBT glasses, which is less than the right-hand side of Equation 9 (taking $\nu_{ph} = 10^{13} \text{ Hz}$), and W_H from Table III), thereby suggesting that non-adiabatic hopping theory is most appropriate for describing polaron hopping condition in the $VB + xBaTiO_3$ (VBBT) glasses. For VB glass, on the other hand, an adiabatic hopping conduction mechanism is observed [4], because the value of ΔE_j (from Equation 10) is estimated to be $\sim 0.293 \text{ eV}$, with a value of $N(E_F) = 7 \times 10^{21} \text{ eV}^{-1} \text{ cm}^{-3}$ and $\epsilon_p = 6.5$, whereas the right-hand side of Equation 9 is $\sim 0.003 \text{ eV}$ with $W_H = 0.21 \text{ eV}$ and $\nu_{ph} = 10^{11} \text{ Hz}$. The value of the small polaron coupling constant, γ_p , which is a measure of the electron–phonon interaction in the VBBT glasses, can be estimated from the relation [20] $\gamma_p = 2W_H/h\nu_{ph}$. The values of γ_p for the VBBT glasses (listed in Table III) are found to vary from

7.05–7.60. Austin and Mott suggested that a value of $\gamma_p > 4$ usually indicates strong electron–phonon interaction in solids. From the values of γ_p , an estimate of the polaron effective mass, m_p , in the VBBT glasses is obtained using the relation [20]

$$m_p = (h/2 \Delta E_j R^2) \exp(\gamma_p) = m^* \exp(\gamma_p) \quad (11)$$

where m^* is the rigid lattice effective mass. The calculated values of γ_p and m_p/m^* are found to be quite large (Table III) indicating strong electron–phonon interaction in these glasses, which also supports the formation of small polarons [31].

Recently, Triberis and Friedman [32, 33] used percolation theory to evaluate the conductivity of disordered materials at high and low temperature. Taking correlation into account, they derived [32, 33] an expression for the d.c. conductivity similar to Mott's expression for VRH conductivity

$$\sigma_{d.c.} = \sigma_0 \exp(-T_0/T)^{1/4} \quad (12)$$

where constants σ_0 and T_0 have different values at high and low temperatures. However, if the correlation is neglected, the temperature dependence of the conductivity reduces to the form

$$\sigma_{d.c.} = \sigma_0 \exp(-T_0/T)^{2/5} \quad (13)$$

The present conductivity data for the VBBT glasses are analysed with the model of Triberis and Friedman; the temperature dependence of d.c. conductivity, as predicted by Equations 12 or 13, has not been observed for the glasses of our present investigation.

Finally, Schnakenberg [34] has also suggested that as the temperature is lowered the multiphonon processes are replaced by a single optical phonon process and, at the lowest temperatures, the polarons hop with one or more acoustic phonons making up the differences between sites. The fall of activation energy with temperature in the intermediate temperature region is expressed by the relation [34]

$$W = W' (\tanh \frac{1}{4} h\omega_{ph} \beta / \frac{1}{4} h\omega_{ph} \beta) \quad (14)$$

where W and W' are the low- and high-temperature activation energies, respectively, $\beta = 1/k_B T$, $\omega_{ph} = 2\pi\nu_{ph}$ and h is the Planck's constant. In Fig. 8a the experimental values of W/W' and also the theoretical values given by Equation 14 are plotted against $1/T$, for a typical $90V_2O_5-10Bi_2O_3$ glass doped with 20 wt % $BaTiO_3$. Other glass samples also show similar behaviour. A similar plot for VB glass is shown in Fig. 8b for comparison. The experimental value of activation energy decreases with decreasing temperature, but the quantitative fit with the theoretical plot of Equation 14 is rather poor. This indicates that the decrease in magnitude of conductivity with temperature cannot be accounted for by the decrease in activation energy alone. Thus the theoretical models of polaronic conduction can qualitatively explain the conductivity data, but fail to give any quantitative agreement for the present glass system.

4. Conclusion

Small polaron theory can explain well the temperature dependence of d.c. conductivity of the $V_2O_5-Bi_2O_3$

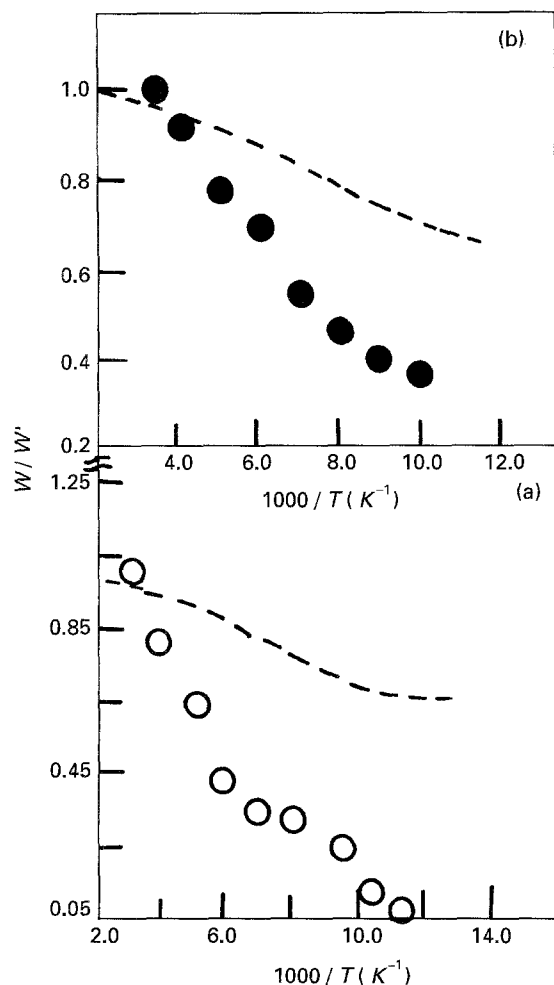


Figure 8 (a) Plot of W/W' as a function of $1/T$ for the $90\text{V}_2\text{O}_5-10\text{Bi}_2\text{O}_3-x\text{BaTiO}_3$ (for $x = 20$ wt %) glass. (—) Theoretical [34] plot, and (○) experimental results. (b) Plot of W/W' as a function of $1/T$ for the $90\text{V}_2\text{O}_5-10\text{Bi}_2\text{O}_3$ glass. (—) Theoretical [34] and (●) experimental points.

and the BaTiO_3 -doped $\text{V}_2\text{O}_5-\text{Bi}_2\text{O}_3$ (VBBT) glasses. At higher temperatures, the adiabatic hopping theory is most appropriate for the $\text{V}_2\text{O}_5-\text{Bi}_2\text{O}_3$ glasses for describing polaronic conduction, while for BaTiO_3 -doped $\text{V}_2\text{O}_5-\text{Bi}_2\text{O}_3$ glasses, non-adiabatic hopping theory is most appropriate. Such a change-over in the conduction mechanism appears to be due to the change of the network structure of the vanadate glasses on the addition of BaTiO_3 . Similar behaviour is also observed for $\text{V}_2\text{O}_5-\text{Bi}_2\text{O}_3$ glasses doped with SrTiO_3 (unpublished). For $\text{V}_2\text{O}_5-\text{Bi}_2\text{O}_3$ glasses with a lower concentration of V_2O_5 , the glass-forming region with BaTiO_3 and SrTiO_3 is less (1–10 wt %). An appreciable change in the mechanism of a.c. conductivity has also taken place in the BaTiO_3 -doped VB glasses [19]. While the correlated barrier hopping model [35] is applicable for the $\text{V}_2\text{O}_5-\text{Bi}_2\text{O}_3$ glasses, an overlapping large polaron tunnelling model [36] is suitable for the BaTiO_3 -doped $\text{V}_2\text{O}_5-\text{Bi}_2\text{O}_3$ glasses. However, in the low-temperature region, for all the glasses (both doped and undoped), conduction takes place by a variable range hopping mechanism.

Acknowledgements

One of the authors (S.C.) thanks the University Grants Commission for financial assistance. The authors

are also grateful to Professor N. Ray Chowdhuri, Professor S. P. Sengupta, Professor B. G. Ghosh and Dr R. Banerjee for providing the facilities to study DTA, SEM, IR, XRD and e.p.r. of the samples, and to Dr K. K. Som for his valuable remarks.

References

1. G. N. GREAVES, *J. Non-Cryst. Solids* **11** (1973) 427.
2. C. H. CHUNG, J. D. MACKENZIE and L. MURAWSKI, *Rev. Chem. Miner.* **16** (1979) 308.
3. C. H. CHUNG and J. D. MACKENZIE, *J. Non-Cryst. Solids* **42** (1980) 151.
4. A. GHOSH and B. K. CHAUDHURI, *ibid.* **83** (1986) 151.
5. H. HIRASHIMA, Y. WATANABE and T. YOSHIDA, *ibid.* **95/96** (1987) 826.
6. J. LIVAGE, J. P. JOLIVET and E. TRONE, *ibid.* **121** (1990) 35.
7. H. GAHLMAN and R. BRUCKNER, *ibid.* **13** (1974) 355.
8. A. GHOSH and B. K. CHAUDHURI, in "Proceedings of the National Seminar on Semiconductor and Devices", Calcutta (1986) p. 28.
9. A. GHOSH, *J. Appl. Phys.* **64** (1988) 2652.
10. Y. SAKURI and J. YAMAKI, *J. Electrochem. Soc.* **12** (1985) 512.
11. S. NAKAMURA and N. ICHINOSE, *J. Non-Cryst. Solids* **94/95** (1987) 849.
12. A. GHOSH and B. K. CHAUDHURI, *J. Mater. Sci.* **22** (1985) 2369.
13. I. G. AUSTIN and N. F. MOTT, *Adv. Phys.* **18** (1969) 41.
14. R. WERNICKLE, in "Grain boundary phenomena in Electronic ceramics", Vol. I, Edited by L. H. Leison (American Ceramic Society) Westerville, OH, 1981) p. 261.
15. SAHANA CHAKRABORTY, A. K. BERA, S. MOLLAH and B. K. CHAUDHURI, *J. Mater. Res.* **9** (1994) 1932.
16. G. ARLT, D. HENNINGS and G. DE WITH, *J. Appl. Phys.* **58** (1985) 1619.
17. K. K. SOM and B. K. CHAUDHURI, *Phys. Rev. B* **41** (1990) 1581.
18. Y. KAWAMOTO, M. FUKUZUKO, Y. OHTA and M. IMAI, *Phys. Chem. Glasses* **20** (1979) 54.
19. S. CHAKRABORTY, S. SADHUKHAN, K. K. SOM, H. S. MAITI and B. K. CHAUDHURI, *Phil. Mag. B* (1995) in press.
20. N. F. MOTT, *J. Non-Cryst. Solids* **1** (1968) 1.
21. M. SAYER and A. MANSINGH, *Phys. Rev. B* **6** (1972) 4629.
22. B. K. CHAUDHURI, K. CHAUDHURI and K. K. SOM, *J. Phys. Chem. Solids* **50** (1989) 1137.
23. C. H. CHUNG and J. D. MACKENZIE, *J. Non-Cryst. Solids* **42** (1980) 357.
24. S. MOLLAH, K. K. SOM, K. BOSE, A. K. CHAKRABORTY and B. K. CHAUDHURI, *Phys. Rev. B* **46** (1992) 11075.
25. I. G. AUSTIN and E. S. GARBETT, in "Electronic and structural properties of amorphous semiconductors", edited by P. G. Lecomber and J. Mort (Academic Press, London, New York) p. 393.
26. T. HOLSTEIN, *Ann. Phys. (N.Y.)* **8** (1959) 325.
27. *Idem*, *ibid.* **8** (1959) 343.
28. V. N. BOGOMOLOV, E. K. KUDINEV and U. N. FIRSOV, *Sov. Phys. Solid State* **9** (1968) 2502; (*Fizika Tverodogo Tela* **9** (1967) 3175).
29. A. MILLER and E. ABRAHAMS, *Phys. Rev.* **120** (1960) 745.
30. D. EMIN and T. HOLSTEIN, *Ann. Phys. (N.Y.)* **53** (1969) 439.
31. N. F. MOTT and E. A. DAVIS, in "Electronic processes in non-crystalline materials", 2nd Ed (Clarendon, Oxford, 1979).
32. G. P. TRIBERIS, *J. Non-Cryst. Solids* **74** (1985) 1.
33. G. P. TRIBERIS and L. R. FRIEDMAN, *J. Phys. C Solid State Phys.* **14** (1981) 4631.
34. J. SCHNAKENBERG, *Phys. Status Solidi* **28** (1968) 623.
35. G. E. PIKE, *Phys. Rev. B* **6** (1972) 1572.
36. A. R. LONG, *Adv. Phys.* **31** (1982) 553.

Received 22 December 1994
and accepted 28 April 1995